

Predicting Martian Dune Characteristics Using Global and Mesoscale MarsWRF Output. Newman¹, C.E., Lancaster², N., Rubin³, D.M. and Richardson⁴, M.I.. ¹Ashima Research, 600 South Lake Ave., Suite 104, Pasadena, CA 91106, USA. claire@ashimaresearch.com. ²Division of Earth and Ecosystem Science, Desert Research Institute, 2215 Raggio Parkway, Reno, NV 89512. Nick.Lancaster@dri.edu. ³USGS Pacific Coastal & Marine Science Center, 400 Natural Bridges Drive, Santa Cruz, CA 95060. drubin@usgs.gov. ⁴Ashima Research, 600 South Lake Ave., Suite 104, Pasadena, CA 91106, USA. mir@ashimaresearch.com.

Introduction: Dune characteristics, when coupled with understanding of dune formation processes, may be used to infer the near-surface circulation at the time of their formation. Relevant characteristics include (though are not limited to) dune location, bedform orientations, inferred resultant transport directions, and dune types. While one approach is to examine observations of dunes and attempt to relate these to dominant or prevailing wind directions *etc.*, another approach is to simulate the full time-varying wind regime over a dune field, couple this with theories of bedform growth and motion, then compare the predicted dune characteristics with those observed. In the latter approach, good agreement provides confidence in the predicted wind regime.

Successful prediction of the characteristics of active dunes would (a) confirm that we understand dune formation processes, and (b) support our predictions of the current wind regime, which is of great benefit for Mars in the absence of near-surface meteorological monitoring. However, inactive dunes may also provide insight into recent climate change on Mars, related to variations in the orbital forcing. For example, the global circulation is predicted to change considerably at high obliquities [1,2], which would in turn produce changes in near-surface wind stress patterns and dune formation. Dune characteristics in disagreement with predictions for the current wind regime may thus be more representative of the circulation during past orbital epochs, and suggest that these dunes are inactive at the present time. We can even model the wind regime under different orbital conditions to gain insight into the conditions under which the dunes formed.

Caveats are of course that (a) we may not yet understand dune formation processes sufficiently well to predict dune characteristics, even given perfect knowledge of the dune-forming wind field, and/or (b) we may not be simulating the dune-forming wind field correctly, particularly under past orbital conditions for which *e.g.* the atmospheric dust forcing is unknown, and for which our models cannot be calibrated (other than with studies such as this). For these reasons, (a) testing and improving our understanding of dune formation processes (via laboratory, field and modeling projects on Earth), and (b) the correct prediction of

Mars dunes known to be currently active, are important validation steps to pursue in future work.

Approach: We performed global and mesoscale simulations using the MarsWRF general circulation model (GCM) to predict the near-surface circulation for different orbital conditions, both globally at 2° resolution and over Gale Crater at ~4km resolution. We then looked at (1) predictions of where saltation thresholds are exceeded, (2) predictions of bedform orientations based on the theory of Gross Bedform-Normal Transport (see below), and (3) predictions of resultant sand transport directions. (1) can be compared to observations of dune locations, though this is complex because, while saltation implies that dunes may be active, it also implies that sand may be removed from a region over time. For example, high saltation rates at a location may suggest an absence of sand altogether, rather than the presence of active dunes. (2) can be compared to observed bedform orientations, while (3) can be compared to observations relating to net dune motion (such as the position of a dune field within a crater, assuming that in the absence of any wind the sand would be more evenly, or at least symmetrically, distributed).

The MarsWRF model: MarsWRF is the Mars version of the planetWRF GCM (publicly available at www.planetwrf.com), developed from NCAR's widely used terrestrial Weather Research and Forecasting (WRF) model [3,4]. MarsWRF is a multi-scale three-dimensional model that can be used for large eddy simulations (*i.e.*, run over small regions at very high resolutions of ~m), standalone mesoscale simulations (*i.e.*, run over a limited area with resolutions of ~100m to ~10km), global simulations (with resolutions of ~0.5° to 5°), or global simulations with high-resolution mesoscale regions embedded ('nested') inside them.

The version of MarsWRF used includes the seasonal and diurnal cycle of solar heating, a correlated-k radiative transfer scheme (which closely matches results produced using line-by-line code [5]), a CO₂ cycle (condensation and sublimation), vertical mixing of heat, dust and momentum according to atmospheric stability, and sub-surface diffusion of heat. MarsWRF also includes prescribed, seasonally-varying atmospheric dust (to mimic say a dust storm year or a year with no major storms) but may also be run with fully

interactive dust using parameterized dust injection that responds self-consistently to changes in the circulation.

For this study we used global MarsWRF both without and with nesting (down to ~ 4 km resolution) over Gale Crater, and using a prescribed atmospheric dust distribution representative of a storm-free year.

Gross Bedform-Normal Transport: We apply the theory of Gross Bedform-Normal Transport (GBNT [6]) to predict dune orientations. This theory revolves around two basic concepts: (i) dunes form in the *long-term* wind field, and (ii) dune orientations are *not* determined by *net* transport, but rather by gross transport in *either* direction across a dune crest. (ii) can be understood if one considers two equal winds, both perpendicular to a dune crest, but carrying sand in opposite directions across it. In a net sense the flux of sand across the dune crest is zero, but since sand fluxes in both directions build the crest it is actually the *gross* sand transport perpendicular to the crest from both directions that should be considered.

The GBNT theory states that bedforms will align such that the total transport across a dune crest is maximized in a given wind field, where ‘total transport’ is the gross bedform-normal transport (GBNT) as demonstrated in Figure 1 for a situation with two primary sand transport directions. In such a simple case the bedform orientation can be calculated analytically, but in general there will be winds of varying strengths in all directions over the course of a Mars year, and the predicted orientation can instead be found by calculating the GBNT for all possible dune orientations (from N-S to S-N, *i.e.* from 0° to 180°), then choosing the orientation for which GBNT is maximized.

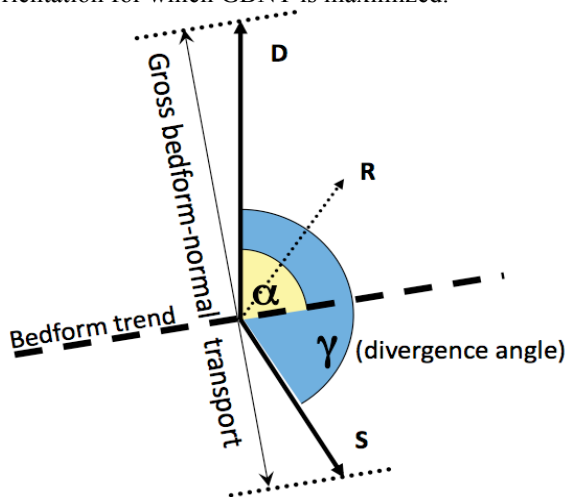


Figure 1: A situation with sand transport in only two wind directions, shown by D (dominant) and S (secondary). Resultant (net) transport is shown by R, but for dune growth it’s the total transport in either direction normal to the bedform (gross bedform-normal transport, GBNT) that is important.

We calculate this by running MarsWRF to predict near-surface winds over a long time period (one or multiple Mars years), outputting every Mars minute, to capture the long-term high-frequency dune-forming wind field. We then choose a saltation threshold and calculate sand fluxes in all directions [0, 1, ...359° from N]. We consider all possible bedform orientations [0, 1, ...179° from N] and sum the gross sand flux perpendicular to each orientation over the entire time period. Finally, we find the orientation for which the total gross flux is maximum (note that secondary maxima also indicate predicted secondary bedform orientations). We repeat this analysis for 8 saltation thresholds, from 0 to 0.049 N/m^2 in steps of 0.007 N/m^2 .

Global results: We ran MarsWRF at 2° global resolution and compared results with dune measurements in the Mars Global Digital Dune Database (MGD³, *e.g.* Hayward *et al.*, 2009).

Dune locations. We can use MarsWRF to predict where saltation should occur over a Mars year, assuming a range of saltation thresholds. However, while the saltation threshold must be exceeded for dunes to form, a complication involves where sand accumulates over the longer term. Regions with high wind stresses may in fact lose their sand over timescales on the order of 100s of years or greater, while sand remains longest in regions where wind stresses are lower. For example, for a saltation threshold of 0.028 N/m^2 we find that the observed northern polar dunes coincide fairly closely with a region predicted to have annual winds always below this threshold (not shown). However, a far more rigorous study of long-term sand transport across the martian surface (indicating regions of sand convergence and divergence) would be required to assess where net sand accumulation should occur.

Bedform orientations. The MGD³ records up to four slipface azimuths for each dune field. Assuming these to be approximately normal to bedform orientations, and initially treating the first recorded slipface as most representative of the overall region, we can compare it to the normal to our predicted bedform orientations at a nearby point in the GCM output. Figure 2 shows an example of results, for present day Mars using a threshold of 0.021 N/m^2 . Green symbols indicate agreement between the predicted and observed bedform orientation; blue symbols indicate no agreement; and red symbols indicate dune locations at which no comparison is possible (see caption for details).

Results vary when the saltation threshold is changed, or when an obliquity of 35° (rather than the current value of $\sim 25^\circ$) is used, but overall we find at most $\sim 50\%$ agreement averaged over all valid locations (*i.e.*, as many or more blue symbols as green) for all conditions examined. Global experiments are ongo-

ing for a wider range of obliquity values and atmospheric dust loadings; also, the agreement is improved if only certain regions are considered. However, more in-depth examination of results (and comparison with mesoscale results, see below) suggests that global scale studies are inadequate when comparing to the majority of dune fields, which are strongly influenced in most cases by local scale topographically-controlled flows.

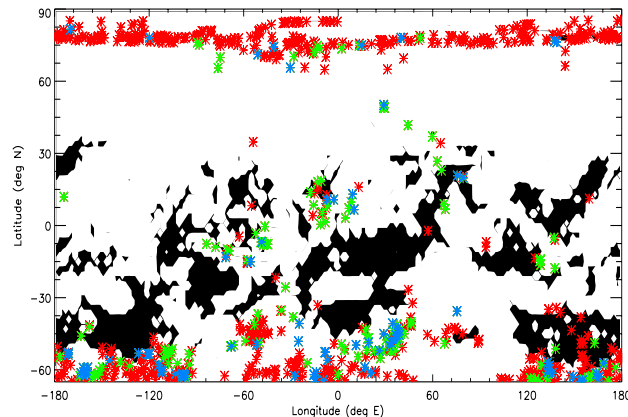


Figure 2: Comparison between observed and predicted bedform orientations (see text for details) for a threshold of 0.021N/m^2 . Green symbols indicate agreement (defined as the GCM-predicted bedform orientations being within 45° of the normal to the first MGD³ slipface azimuth); blue symbols indicate no agreement; and red symbols indicate dune locations with no comparison possible, *i.e.*, with no measured slip faces, or with no saltation predicted in the GCM for this threshold (such GCM locations are shown as black).

Inferred resultant transport directions. Dune movement is sometimes considered as either migration of the dune (movement perpendicular to its crest) and elongation of the dune (movement in the direction of its crest). It is reasonable to assume that the combination of these two movements produces an overall translation of dunes in the direction of resultant (net) transport (as indicated by R in Figure 1). The MGD³ gives a ‘dune centroid azimuth’ (DCA) for dunes located in craters, which indicates the position of the dunes relative to the crater centroid. We assume that this direction should indicate the translation direction of the dunes, and compare data on this to our model predictions of resultant transport direction.

As with bedform orientations, we find at most $\sim 50\%$ agreement between observations and predictions averaged over all valid points for all thresholds and obliquities considered. As an example, Figure 3 shows results for the present day, again using a threshold of 0.021N/m^2 . Although the agreement % changes if we bin results according to crater size, further examination of results and comparison with mesoscale simulations

suggests again that higher resolutions are required to properly capture the dune forming winds.

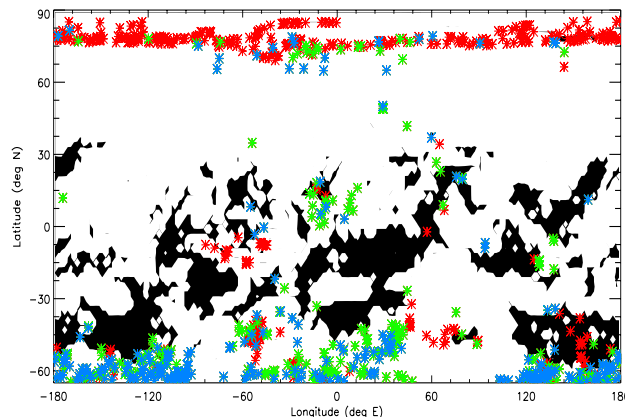


Figure 3: As in Figure 2, but now showing the agreement between inferred and predicted resultant transport directions.

Mesoscale results: Figure 4 shows the predicted bedform orientations and resultant transport directions, assuming a threshold of 0N/m^2 , for a present day $\sim 4\text{km}$ resolution mesoscale simulation of Gale Crater.

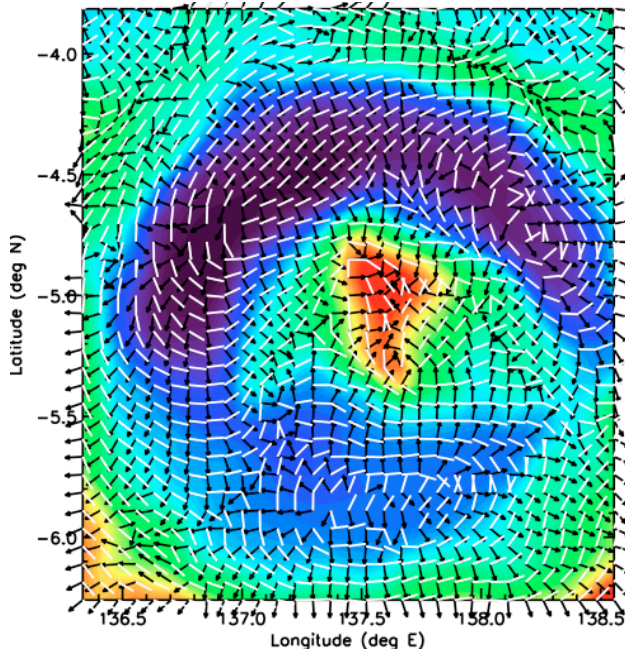


Figure 4: Contours show Gale Crater topography (purple is low, red is high). See text for further details.

Figure 5 focuses on the lowest-lying dune field in the crater (right hand plot) and shows the impact on predicted resultant transport direction and bedform orientation of varying the saltation threshold. For a saltation threshold of 0 (left plot) the predicted dunes are oriented between $\sim\text{NNW-SSE}$ and $\sim\text{E-W}$, and range from oblique (bedform orientation and resultant

between 15 and 75° of each other) to transverse (bedform orientation and resultant between 75 and 90° of each other). However, the observed dunes (right plot) are typically oriented ~NNE-SSW. (Note the white arrows in the right plot show slipfaces, which are ~90° to the dune crests, and should not be compared with the resultant transport vectors predicted by the GCM).

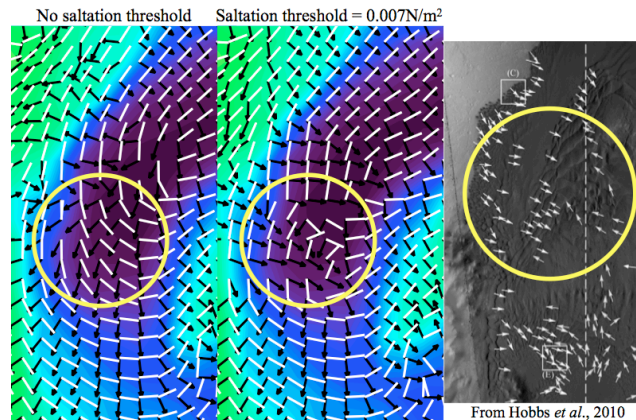


Figure 5: Predicted bedform orientations (white lines) and resultant transport directions (black arrows) for the present day, using a saltation threshold of 0 (left plot) and 0.007N/m² (middle plot). For comparison the observed dunes and measured slipface orientations (white arrows), which are ~normal to the observed bedform orientations, are shown in the right plot. The yellow circles show the same location in all plots.

If we increase the saltation threshold to 0.007N/m² (middle plot), however, we predict dune orientations of ~NNE-SSW, as observed, and also predict an increase in the fraction of transverse dunes. Further detailed comparison is required to assess whether the predicted dune morphologies are consistent with those observed, and this experiment will also be repeated using different atmospheric dust loadings and at higher resolution to assess the robustness and validity of results.

Figure 6 shows the impact of further increasing the threshold and of running the GCM at higher obliquity. Focusing just south of the region originally highlighted, it can be seen that changing the obliquity has little impact for a low threshold, whereas raising the threshold alone extends the ~NNE-SSW region further south, and increasing the obliquity at this higher threshold enables saltation thresholds to be exceeded over a greater fraction of the crater interior.

Further work: These investigations have demonstrated the importance of using sufficiently high resolution for Mars dune studies, and preliminary Gale Crater results suggest that matching observations to predictions could indicate the saltation thresholds and even potentially the orbital configuration at which dunes formed; however, only a few scenarios (dust

loading and/or obliquity) have been examined to date, and significant further work is required – including higher resolution simulations and a closer examination of the observed dune orientations and morphologies – before any firm conclusions can be drawn. We will also be expanding these mesoscale studies to other regions, including those in which dune migration has been observed over recent years (*e.g.*, Nili Patera [7]). Dune migration indicates that dunes are currently active and suggests that these bedforms are in equilibrium with the current wind regime. This enables us to compare their characteristics with model predictions for the present day climate without needing to consider other orbital settings, and hence provides a means of validating our approach.

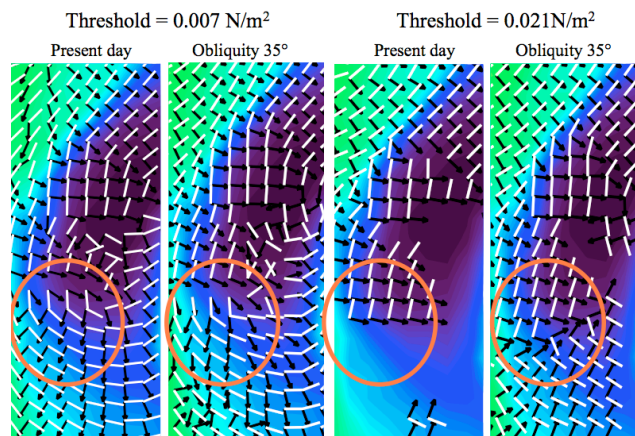


Figure 6: As Figure 5 but for two thresholds: 0.007 (left two plots) and 0.021N/m² (right two plots); and for two obliquities: ~25° (present; 1st and 3rd plot) and 35° (2nd and 4th plot).

References: [1] Haberle *et al.* (2003) *Icarus*, 161, 66-89. [2] Newman *et al.* (2005) *Icarus*, 174, 135-160. [3] Richardson *et al.* (2007) *J. Geophys. Res.*, 112, doi:10.1029/2006JE002825. [4] Toigo *et al.* (2012) *Icarus*, accepted. [5] Mischna *et al.* (2012) *J. Geophys. Res.*, in review. [6] Rubin D. M. and Hunter R. E. (1987) *Science*, 237, 276–278. [7] Bridges *et al.* (2012) *Nature*, 485, 339–342.